



Formation of Nuclear Disks and Supermassive Black Hole Binaries in Galaxy Mergers

L. Mayer,^{1,2} S. Kazantzidis,³ and A. Escala⁴

¹ Institute for Theoretical Physics, University of Zürich, Winterthurestrasse 190, CH-8057 Zürich, Switzerland

² Institut für Astronomie, ETH Zürich, Wolfgang-Pauli-Strasse 16, CH-8093 Zürich, Switzerland

³ Center for Cosmology and Astro-Particle Physics, The Ohio State University, 191 West Woodruff Avenue, Columbus, OH 43210, USA

⁴ Kavli Institute for Particle Astrophysics and Cosmology, Stanford University, P.O. Box 20450, MS 29, Stanford, CA 94309 USA

Abstract. We review the results of the first multi-scale, hydrodynamical simulations of mergers between galaxies with central supermassive black holes (SMBHs). We demonstrate that strong gas inflows due to tidal torques produce nuclear disks at the centers of merger remnants whose properties depend sensitively on the details of gas thermodynamics. We show that a SMBH binary forms very rapidly, less than a million years after the merger of the two galaxies, owing to the drag exerted by the surrounding gaseous nuclear disk. Binary formation is significantly suppressed in the presence of a strong heating source such as radiative feedback by the accreting SMBHs. We also present preliminary results of numerical simulations with ultra-high spatial resolution of 0.1 pc in the gas component. These simulations resolve the internal structure of the resulting nuclear disk down to parsec scales and demonstrate the formation of a central massive object ($\sim 10^8 M_\odot$) by efficient angular momentum transport due to the disk's extended spiral arms. Due to the rapid formation of the central clump, the density of the nuclear disk decreases significantly in its outer region, reducing dramatically the effect of dynamical friction and leading to the stalling of the two SMBHs at a separation of ~ 1 pc. We discuss how the orbital decay of the black holes might continue in a more realistic model which incorporates star formation and the multi-phase nature of the ISM.

Key words. Galaxies: Mergers – Galaxies: Structure – Black Holes: Evolution – Black Holes: Binaries – Cosmology: Theory – Methods: Numerical

1. Introduction

In recent years, compelling dynamical evidence has indicated that supermassive black holes (SMBHs) are ubiquitous in galactic nu-

clei (e.g., Ferrarese & Ford 2005). According to the standard modern theory of cosmological structure formation, the Cold Dark Matter (CDM) paradigm (e.g., Blumenthal et al. 1984), galaxies in the Universe grow through a complex process of continuous mergers and

Send offprint requests to: L. Mayer

agglomeration of smaller systems. Thus, if more than one of the protogalactic fragments contained a SMBH, the formation of SMBH binaries during galaxy assembly will be almost inevitable (e.g., Begelman et al. 1980).

In a purely stellar background, as the binary separation decays, the effectiveness of dynamical friction slowly declines, and the pair can become tightly bound via three-body interactions, namely by capturing stars that pass close to the black holes and ejecting them at much higher velocities (e.g., Milosavljević & Merritt 2001). If the hardening continues to sufficiently small relative distances, gravitational wave emission becomes the dominant source of orbital energy loss and the two SMBHs may coalesce in less than a Hubble time. However, the binary orbit may stop shrinking before gravitational radiation becomes relevant as there is a finite supply of stars on intersecting orbits (e.g., Berczik et al. 2005).

During the assembly of galaxies, especially at high z , their SMBHs likely evolve within gas-rich environments. Merging systems such as the Ultraluminous Infrared Galaxies (ULIRGs) NGC 6240 and Arp 220 harbor large concentrations of gas, in excess of $10^9 M_\odot$, at their center, in the form of either a turbulent irregular structure or of a kinematically coherent, rotating disk (e.g., Downes & Solomon 1998). Massive rotating nuclear disks of molecular gas are also ubiquitous in galaxies that appear to have just undergone a major merger, such as Markarian 231 (Davies et al. 2004). Gas dynamics may thus profoundly affect the pairing of SMBHs both during and after their host galaxies merge (e.g., Escala et al. 2004; Kazantzidis et al. 2005).

Recent simulations of the orbital evolution of SMBHs within an equilibrium, rotationally-supported, gaseous disk have shown that dynamical friction against the gaseous background leads to the formation of a tightly bound SMBH binary with a final separation of < 1 pc in about 10^7 yr (Escala et al. 2005; Dotti et al. 2006; Dotti et al., these proceedings). Here we review the results of high-resolution N -body + smoothed particle hydrodynamics (SPH) simulations of mergers between galax-

ies with central SMBHs having enough dynamic range to follow the black holes from hundreds of kiloparsecs down to sub-parsec scales, bridging more than ten orders of magnitude in density.

2. Methods

The aim of this study is to investigate the orbital evolution and pairing of SMBHs in multi-scale galaxy mergers in the hydrodynamical regime. A thorough description of our methods is presented in Kazantzidis et al. (2005) and Mayer et al. (2007, hereafter M07) and we summarize them here. First, we started with two identical spiral galaxies, comprising a disk of stars and gas with an exponential surface density distribution, a spherical, non-rotating Hernquist bulge, and a spherical and isotropic NFW dark matter halo. We adopted parameters from the Milky Way model A1 of Klypin et al. (2002) to initialize the galaxy models.

Specifically, the dark matter halo had a virial mass of $M_{\text{vir}} = 10^{12} M_\odot$, a concentration parameter of $c = 12$, and a dimensionless spin parameter of $\lambda = 0.031$. The mass, thickness and resulting scale length of the disk were $M_d = 0.04 M_{\text{vir}}$, $z_0 = 0.1 R_d$, and $R_d = 3.5$ kpc, respectively. The bulge mass and scale radius were $M_b = 0.008 M_{\text{vir}}$ and $a = 0.2 R_d$, respectively. The halo was adiabatically contracted to respond to the growth of the disk and bulge resulting in a model with a central total density slope close to isothermal. The galaxy models were consistent with the stellar mass Tully-Fisher and size-mass relations. A softened particle of mass $2.6 \times 10^6 M_\odot$ was placed at the center of the bulge to represent a SMBH. This choice satisfies the $M_{\text{BH}} - \sigma$ relation (Kazantzidis et al. 2005). Lastly, the gas fraction, f_g , was chosen to be 10% of the total disk mass. We used a standard cooling function for a primordial mixture of atomic hydrogen and helium. We also shut off radiative cooling at temperatures below 2×10^4 K that is a factor of ~ 2 higher than the temperature at which atomic radiative cooling would drop sharply due to the adopted cooling function. With this choice we effectively take into ac-

count non-thermal, turbulent pressure to model the warm ISM of a real galaxy.

The galaxies were placed on parabolic orbits with pericentric distances that were 20% of the halo virial radius ($r_{\text{peri}} \sim 50$ kpc), typical of cosmological mergers (e.g., Khochfar & Burkert 2006). The initial separation of the halo centers was twice their virial radii and their initial relative velocity was determined from the corresponding Keplerian orbit of two point masses. Each galaxy consisted of 10^5 stellar disk particles, 10^5 bulge particles, and 10^6 dark matter particles. The gas component was represented by 10^5 particles. We employed a gravitational softening of $\epsilon = 100$ pc for both the dark matter and baryonic particles of the galaxy, and $\epsilon = 30$ pc for the particle representing the SMBH.

During the interaction between the two galaxies, the relative separation of the black holes followed that of the galactic cores in which they were embedded. The merging galaxies approached each other several times as they sank into one another via dynamical friction. After ~ 5 Gyr, the dark matter halos had nearly merged and the two baryonic cores, separated by about 6 kpc, continued to spiral down. As much as 60% of the gas originally present in the galaxies was funneled to the inner few hundred parsecs of each core by tidal torques and shocks occurring in the repeated fly-bys between the two galaxies (e.g., Barnes & Hernquist 1996). Each SMBH was embedded in a rotating gaseous disk of mass $\sim 4 \times 10^8 M_{\odot}$ and size of a few hundred parsecs which was produced by the gas inflow.

Second, just before the last pericentric passage of the two merging galaxies, we adopted the technique of particle splitting to increase the gas mass resolution in the central region of the computational volume. By selecting a large enough volume for the fine grained region one can avoid dealing with spurious effects at the coarse/fine boundary, such as two-body heating due to scattering by massive particles of the low-resolution region. We selected the volume of the fine-grained region to be large enough to guarantee that the dynamical timescales of the entire coarse-grained region were much longer than those corresponding to the refined region.

Specifically, we performed the splitting in a volume of 30 kpc in radius at the point where the two galaxy cores were separated by only 6 kpc. The new particles were randomly distributed according to the SPH smoothing kernel within a volume of size $\sim h_p^3$, where h_p is the smoothing length of the parent particle. The velocities of the child particles were equal to those of their parent particle (ensuring momentum conservation) and so was their temperature, while each child particle was assigned a mass equal to $1/N_{\text{split}}$ the mass of the parent particle, where N_{split} is the number of child particles per parent particle. The mass resolution in the gas component was originally $2 \times 10^4 M_{\odot}$ and became $\sim 3000 M_{\odot}$ after splitting, for a total of ~ 1.5 million SPH particles. For the standard calculations, the softening of the gas particles was set to 2 pc. We note that the local Jeans length was always resolved by 10 or more SPH smoothing kernels (e.g., Bate & Burkert 1997) in the highest density regions of the refined simulations. The softening of the black holes was also reduced from 30 pc to 2 pc, while the softening of dark matter and stellar particles remained 100 pc as they were not split in order to limit the computational burden. Therefore, stellar and dark matter particles essentially provide a smooth background potential, while the computation focused on the gas component which dominates by mass the nuclear region. All simulations were performed with GASOLINE, a multi-stepping, parallel Tree-SPH N -body code (Wadsley et al. 2004).

The radiation physics in the refined simulations was modeled via an “effective” equation of state that accounts for the net balance of radiative heating and cooling. The value of the adiabatic index, γ , namely the ratio between the specific heats, is the parameter that controls the degree of dissipation in the gas. While the various cooling and heating mechanisms should be followed directly, this simple scheme allows us to investigate the effect of thermodynamics on the structure of the merger remnant and on the orbital decay of the black holes.

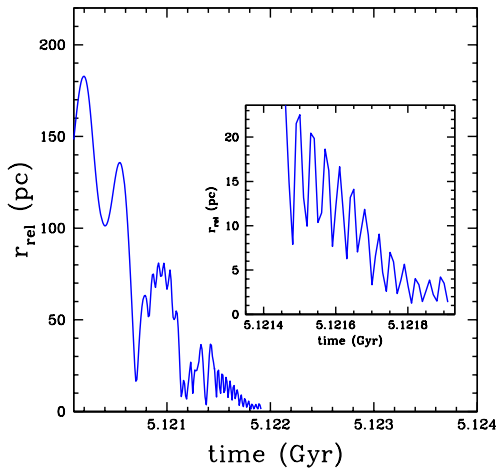


Fig. 1. Relative separation of the two SMBHs as a function of time during the last stage of the standard, multi-scale merger simulation with $\gamma = 7/5$. This value of γ approximates well the balance between radiative heating and cooling in a starburst galaxy. The two peaks at scales of tens of parsecs at around $t = 5.1213$ Gyr correspond to the end of the phase during which each black hole is still embedded in a distinct gaseous core. The inset shows the details of the last part of the orbital evolution, which takes place inside the nuclear disk arising from the merger of the two galactic cores. A SMBH binary forms rapidly, less than a million years after the coalescence of the two galactic nuclei, owing to the drag exerted by the surrounding dense gaseous nuclear disk.

3. Effects of thermodynamics on the orbital decay of SMBHs

Calculations that include radiative transfer show that the thermodynamic state of a solar metallicity gas heated by a starburst can be well approximated by an ideal gas with adiabatic index $\gamma = 1.3 - 1.4$ over a wide range of densities (Spaans & Silk 2000). For the standard refined simulation discussed in the present work, we adopted $\gamma = 7/5$.

The gaseous cores finally merge at $t \sim 5.12$ Gyr, forming a single nuclear disk with a mass of $3 \times 10^9 M_\odot$ and a size of ~ 75 pc. The two SMBHs are embedded in this nuclear disk. The disk is surrounded by several rings and by a more diffuse, rotationally-supported

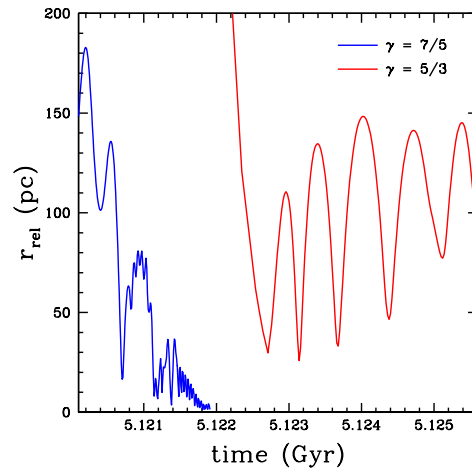


Fig. 2. Relative separation of the two SMBHs as a function of time in two multi-scale, merger simulations with different prescriptions for the gas thermodynamics. The stiffer equation of state ($\gamma = 5/3$) corresponds to a situation where radiative cooling is completely suppressed by a strong heating source (e.g., AGN feedback) and causes the hardening process to significantly slow down. The orbital decay and pairing of SMBHs depends sensitively on the details of gas thermodynamics.

envelope extending out to more than a kiloparsec. A background of dark matter and stars distributed in a spheroid is also present but the gas component is dominant in mass within a few hundred pc from the center. From here on the orbital decay of the black holes is dominated by dynamical friction against this fairly dense gaseous disk. The black holes are on eccentric orbits and move with a speed of $v_{\text{BH}} \sim 200 - 300 \text{ km s}^{-1}$ relative to the disk's center of mass. The typical ambient sound speed is $v_s \sim 50 \text{ km s}^{-1}$. The relative orbit of the SMBH pair decays from about 40 pc to a few parsecs, our resolution limit, in less than a million years after the merger of the two galaxies (Figure 1). At this point the two black holes are gravitationally bound to each other, as the gas mass enclosed within their separation is less than the mass of the binary. Dynamical friction against the stellar background would bring the two black holes this close only on a much longer timescale, $\sim 3 \times 10^7$ yr (Section

4). Such a short sinking timescale due to the gas is expected because of the high densities in the nuclear disk and because the decay occurs in the supersonic regime with $v_{\text{BH}} > v_s$ (Ostriker 1999). The subsequent hardening of the binary will depend on the details of gasdynamics and other processes at scales below the adopted resolution (Sections 6 & 7).

It is interesting to investigate the effect of the adopted equation of state on the orbital decay of the black holes. In particular, we considered a smaller degree of dissipation in the gas and increased γ to $5/3$. This value of γ would correspond to a purely adiabatic gas, or equivalently to a situation where radiative cooling is completely suppressed. The radiative feedback from an active galactic nucleus (AGN) is a good candidate for such a strong heating source. In this case, we find that a turbulent, pressure supported cloud of a few hundred parsecs arises from the merger rather than a disk. The nuclear region is still gas dominated, but the gas mass is lower within 100 pc relative to the $\gamma = 7/5$ case. This is because of the adiabatic expansion of the gas following the final shock when the two cores merged.

Figure 2 demonstrates that the hardening process is significantly suppressed when a stiffer equation of state with $\gamma = 5/3$ is adopted. In this case, the black holes do not form a binary and maintain a relative separation of $\sim 100 - 150$ pc well after the binary forms in the simulation with $\gamma = 7/5$. The density of the gas in the nuclear region surrounding the SMBHs is a factor of ~ 5 lower compared to that in the $\gamma = 7/5$ case, the sound speed is $v_s \sim 100 \text{ km s}^{-1}$, and the black hole velocity is $v_{\text{BH}} \lesssim 100 \text{ km s}^{-1}$. The lower density and to a lesser extent the fact that the two black holes move subsonically ($v_{\text{BH}} \lesssim v_s$) rather than supersonically greatly reduce the drag due to the gas distribution when $\gamma = 5/3$ (Ostriker 1999). In Section 5, we briefly discuss how the structure and kinematics of the nuclear regions of merger remnants in the simulations with different values of γ compare to those of observed systems.

Given the sensitivity of the black hole pairing process to the value of γ , a scenario in which the black holes rapidly form a binary

owing to dynamical friction against the gas would require that AGN feedback has negligible thermodynamical effects on small scales. In fact, this may be a more general requirement if the ubiquitous nuclear disk-like structures seen in many merger remnants are to be preserved. Interestingly, previous studies that included a prescription for AGN feedback in similar galaxy merger simulations (e.g., Springel et al. 2005) find that feedback affects strongly the thermodynamics of the gas in the nuclear region only $> 10^8$ yr after the galaxy merger is completed.

4. Dynamical friction timescales

It is important to examine if the black holes could still form a binary as a result of the interaction with the collisionless stellar background. Since the resolution of the collisionless components is likely inadequate to assess directly the effect of dynamical friction (Section 2), we opt to calculate the dynamical friction timescale in the collisionless background analytically (Colpi et al. 1999)

$$\tau_{\text{DF}} = 1.2 \frac{V_{\text{cir}} r_{\text{cir}}^2}{GM_{\text{BH}} \ln(M_{\text{sd}}/M_{\text{BH}})} \varepsilon^{0.4}. \quad (1)$$

Here V_{cir} and r_{cir} are, respectively, the initial orbital velocity and the radius of the circular orbit with the same energy of the actual orbit of the black holes in the simulation, ε is the circularity of the orbit, and M_{sd} is the sum of the dark matter and stellar mass within r_{cir} .

We calculate the decay time when the two black holes are separated by 100 pc, that is at the periphery of the nuclear disk just after the galaxy merger. Drawing the numbers from the simulations, we have $r_{\text{cir}} = 100$ pc, $V_{\text{circ}} = 200 \text{ km s}^{-1}$, $\varepsilon = 0.5$, $M_{\text{BH}} = 2.6 \times 10^6 M_{\odot}$ and $M_{\text{sd}} = 5 \times 10^8 M_{\odot}$. We find that the dynamical friction timescales in the collisionless background are equal to 5×10^7 yr and 3×10^7 yr in the $\gamma = 5/3$ and $\gamma = 7/5$ simulations, respectively (the shorter timescale in the $\gamma = 7/5$ case is due to the fact that the stars and halo contract adiabatically more in response to the higher gas mass concentration in this case, and hence M_{sd} is higher). In comparison, the binary

formation timescale in the simulation with $\gamma = 7/5$ was only 5×10^5 yr (Figure 1).

We stress that eq. (1) was derived for an isothermal sphere. The stellar and dark matter distribution are indeed only mildly triaxial within a few hundred parsecs from the center of the remnant and the total density profile is fairly close to $\rho(r) \propto r^{-2}$, as expected from previous work (e.g., Kazantzidis et al. 2005). We also note that eq. (1) actually yields a lower limit to the dynamical friction timescale since close to parsec scales, as the binary becomes hard, evacuation of the stellar background due to three-body encounters will take place and the efficiency of the sinking process will be greatly reduced. Whether orbital decay will continue and eventually lead to coalescence of the two black holes is uncertain in this case. Centrophilic orbits in triaxial systems could help in refilling the loss cone and decrease the binary's separation to the point where the emission of gravitational waves becomes efficient at extracting the last remaining angular momentum (Berczik et al. 2005). However, as we just mentioned, the structure of the stellar core is only mildly triaxial. Further investigation with simulations having higher resolution in the collisionless component is needed. The $\gamma = 5/3$ run was stopped 5×10^6 yr after the merger of the gaseous cores is completed. Once again, the fact that there is no evidence that the black holes are sinking until the end is likely due to insufficient mass and force resolution in the collisionless background that does not allow to resolve dynamical friction properly.

We also compared our results with the *expected* dynamical friction timescale due to the gaseous background. In the simulation with $\gamma = 7/5$, the gas is distributed in a disk rather than in an isothermal sphere. Since the disk thickness is > 10 times the black hole gravitational softening and because of the fact that the density profile of the disk can be roughly approximated with a power law with an index close to 2 (except at the center where it becomes steeper) we are allowed to use eq. (1) to obtain a rough estimate of the timescales. As shown by Escala et al. (2004), analytical predictions with a fixed Coulomb logarithm (Ostriker 1999) can overestimate the drag in

the supersonic regime by a factor of ~ 1.5 . In the $\gamma = 7/5$ simulation, the black holes move supersonically and the analytical formula should yield the correct prediction. In this case the drag is a factor of ~ 2.3 stronger than in the corresponding collisionless case (Escala et al. 2004). This is fairly consistent with our results. Indeed, eq. (1) with a reduction of a factor of 2.3 gives $\sim 10^6$ yr if we set $M_{\text{gas}} = M_{\text{sd}}$, with $M_{\text{gas}} \sim 20M_{\text{stars}}$. This timescale has to be compared with that measured directly in the simulation, 5×10^5 yr. As discussed above, the gas profile is actually steeper than r^{-2} near the center. Thus, it is not surprising that the decay is faster. Despite the apparent agreement with the analytically estimated drag, we note that the orbital evolution of the two black holes might be affected by more than just the gravitational wake. Indeed, the nuclear disks show strong, highly dynamical non-axisymmetric structures such as spiral arms (see Section 7) which are highly efficient at removing angular momentum from the orbiting SMBHs.

The drag drops rapidly by an order of magnitude in the subsonic regime (Escala et al. 2004). This coupled with the fact that M_{gas} is a factor of ~ 5 lower in the simulation with $\gamma = 5/3$ compared to that with $\gamma = 7/5$ would give a drag 50 times smaller or $\tau_{\text{DF}} \sim 5 \times 10^7$ yr, explaining why the orbital decay caused by the gas is so inefficient in this case. Thus, in the $\gamma = 5/3$ simulation stars and gas contribute to the drag in a comparable way.

Adding star formation is unlikely to change the above conclusions in any significant way. The unrefined galaxy merger simulation yields a starburst timescale of $\sim 5 \times 10^7$ yr. During this time, which is much longer than the binary formation timescale in the run with $\gamma = 7/5$, half of the gas in the nuclear disk will be turned into stars. Instead, due to the fact that the black hole sinking timescale is comparable to that of the star formation timescale in the $\gamma = 5/3$ simulation, the overall orbital evolution will be dictated by the stars rather than by the gas. There are, however, some caveats in the argument regarding the role of star formation in the $\gamma = 7/5$ case. First, the starburst timescale is based on the unrefined merger simulations. Had we

included star formation in the refined simulations we would have probably found shorter timescales locally since these simulations can resolve much higher densities and the star formation rate depends on the local gas density. Second, one might wonder how the inclusion of feedback from star formation, which was neglected in the unrefined merger simulations, would affect gas properties and, consequently, the orbital decay of the black holes. We defer a detailed numerical study of these considerations to future work.

5. Structure, kinematics, and gas inflow in the nuclear regions of merger remnants

The nuclear disk produced in the $\gamma = 7/5$ case is highly turbulent. The sources of turbulence are the prominent shocks generated as the cores merge and the persistent non-axisymmetric structures sustained by the self-gravity of the disk after the merger is completed (e.g., Wada & Norman 2002). The perturbation due to the black hole binary is a negligible effect since its mass is about 10^3 times smaller than the mass of the disk. The degree of turbulence, of order $50 - 100 \text{ km s}^{-1}$ as measured by the radial velocity dispersion, is comparable to that of observed circumnuclear disks (e.g., Downes & Solomon 1998). The disk is composed by a very dense, compact region of size about 25 pc which contains half of its mass (the mean density inside this region is $> 10^5 \text{ atoms/cm}^3$). The outer region instead, from 25 to 75–80 pc, has a density 10–100 times lower, and is surrounded by even lower-density rotating rings extending out to a few hundred parsecs. The disk scale height also increases from inside out, ranging from 20 pc to nearly 40 pc. The volume-weighted density within 100 pc is in the range $10^3 - 10^4 \text{ atoms/cm}^3$, comparable to that of observed nuclear disks (e.g., Downes & Solomon 1998). This suggests that the degree of dissipation implied by the equation of state with $\gamma = 7/5$ is reasonable despite the simplicity of the thermodynamical scheme adopted.

The rotating, flattened cloud produced in the $\gamma = 5/3$ is instead more turbulent and

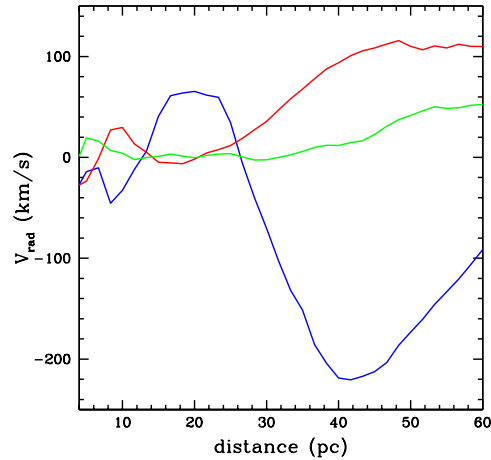


Fig. 3. Radial velocities inside the nuclear disk in the standard, multi-scale merger simulation with $\gamma = 7/5$. The blue line corresponds to $t = 5.1218 \text{ Gyr}$, while red and green lines show results after 10^5 yr and $2 \times 10^5 \text{ yr}$, respectively. Remarkable gas inflows and outflows are the result of streaming motions within the bar and spiral arms. These arise during the phases of strong, non-axisymmetric instabilities sustained by the disk self-gravity. At late times, the instabilities saturate due to self-regulation and the radial motions also decrease.

less dense than observed circumnuclear disks in merger remnants. The mean velocity dispersion measured within 100 pc is about 300 km s^{-1} , higher than the mean rotational velocity within the same radius, which is $\sim 250 \text{ km s}^{-1}$. This suggests that the $\gamma = 5/3$ simulation does not describe the typical nuclear structure resulting from a dissipative merger.

The strong spiral pattern associated with the nuclear disk in the simulation with $\gamma = 7/5$ produces remarkable radial velocities (Figure 3). Since spiral modes transfer angular momentum inwards and mass outwards, strong inward radial velocities are expected. The amplitude of radial motions evolves with the amplitude of the spiral pattern; radial motions decline as the spiral arms weaken over time. Just after the merger, when non-axisymmetry is strongest, radial motions reach amplitudes of $\sim 100 \text{ km s}^{-1}$ (Figure 3). This phase lasts only for a couple of orbital periods, while later

the disk becomes smoother as spiral shocks increase the internal energy which in turn weakens the spiral pattern. Inward radial velocities of order $30 - 50 \text{ km s}^{-1}$ are seen for the remaining few orbital times during which we are able to follow the system (Figure 3). Such velocities are comparable to those recently reported in high-resolution observations of nuclear disks of nearby Seyfert galaxies (Fathi et al. 2006). As the gas reaches down to a distance of few parsecs from the center, its radial velocity diminishes as we approach the resolution limit of the simulations ($\sim 2 \text{ pc}$). Therefore, the fact that there is almost no net radial velocity within a few parsecs from the center (Figure 3) is an artifact of the limited numerical resolution.

If we assume that speeds of $30 - 50 \text{ km s}^{-1}$ can be sustained down to scales of a few parsecs, more than $10^8 M_\odot$ of gas could reach parsec scales in about 10^5 yr . This timescale is much smaller than the duration of the starburst, and therefore such gas inflow should develop in a similar way even when star formation is taken into account. The inflow is also marginally faster than the decay timescale of the binary SMBH measured in the simulation ($\sim 5 \times 10^5 \text{ yr}$). Presumably some of this gas could be intercepted by the two SMBHs as they are spiraling down (the relative velocities between the gas and the black holes are small since the SMBHs are always corotating with the nuclear disk)

6. Merger simulations at sub-pc scales; nuclear fueling and orbital decay of SMBHs

In the study of M07, the simulations were stopped when the two black holes had a separation of about 2 pc , comparable to the adopted gravitational softening length, which sets the nominal resolution limit. At this stage, the black holes had formed a loose binary on a fairly eccentric orbit. In order to explore the sinking of the SMBH binary to even smaller scales we performed a new simulation with a spatial resolution in the gas component of 0.1 pc , that is 20 times higher compared to M07. This resolution is comparable to the highest resolution achieved in simulations of

nuclear disks starting from equilibrium initial conditions rather than from a large scale galaxy merger (Escala et al. 2005; Dotti et al. 2007). On the other hand, the mass resolution in the new simulation was kept the same as in M07. The number of gas particles in the nuclear disk forming after the merger is sufficiently high ($\sim 10^6$) that even with 0.1 pc resolution in the gas the Jeans mass is resolved by several SPH kernels in the disk, thus avoiding spurious numerical effects such as artificial fragmentation (Bate & Burkert 1997).

Due to the much higher spatial resolution, the nuclear disk now reveals a much richer structure with both large and small scale spiral patterns (Figure 4). While the large scale spiral structure was also reported in the simulations of M07, the inner few 10 pc , that were quite featureless before, now reveal a high order spiral pattern extending down to sub-parsec scales. The spirals-in-spirals patterns are reminiscent of the bars-in-bars patterns that are suggested as possible candidates for bridging large and small scale inflows in non-interacting galaxies.

Up to the point when the SMBHs reach a relative separation of $1 - 2 \text{ pc}$ the sinking rate is comparable to what was previously reported by M07. However, at smaller relative separations, the binary's orbital decay slows down and the orbit oscillates between a fraction of a parsec and $\sim 1 \text{ pc}$ (Figure 5). What causes this relative stalling? The answer lies in the evolution of the gas density and temperature profile in the nuclear disk. In a few 10^5 yr , the strong gas inflow produces a very dense central clump with a mass of $\sim 10^8 M_\odot$ and size of only 0.5 pc . We note that this constitutes the first demonstration that a galaxy merger can produce remarkable concentrations of gas at sub-parsec scales subsequent to the formation of a nuclear disk from a larger scale gas inflow. While the density in the very center goes up by an order of magnitude as the central clump forms, at scales above 1 pc the density decreases as angular momentum is transported outwards leading to the expansion of the disk. The disk exhibits a strong non-axisymmetric structure, with multi-armed spirals, extending down to the inner few tens of parsecs (Figure 4). The inner spiral pattern is

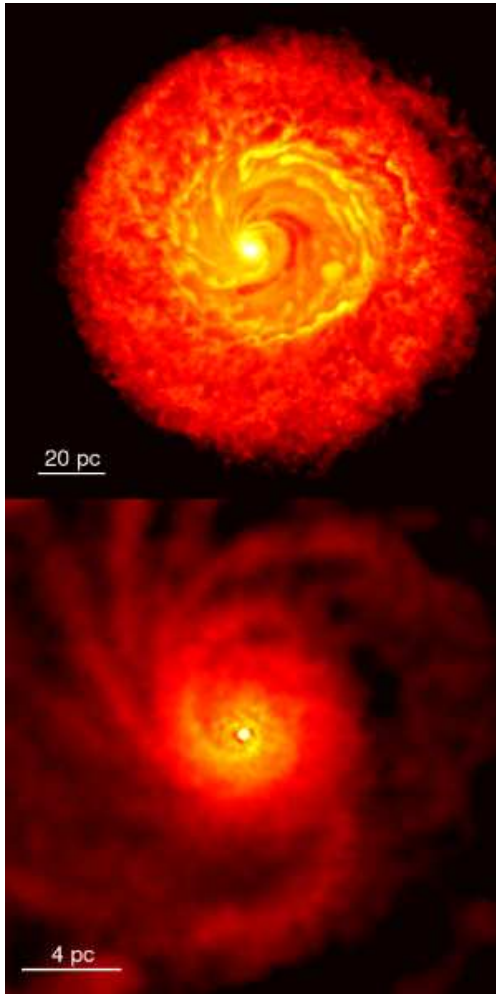


Fig. 4. Color-coded projected density maps of the nuclear disk viewed face-on in the numerical simulation with $\gamma = 7/5$ and 0.1 pc spatial resolution in the gas. Both panels display the nuclear disk $\sim 10^6$ yr after the galaxy merger is deemed complete. The bottom panel presents the inner region of the disk. A conspicuous spiral pattern reaching to the central region and a central, massive clump produced by the strong gas inflow are evident.

responsible for the efficient transfer of angular momentum in the inner disk region and is probably due to the SLING mechanism (Adams et al. 1989; Krumholz et al. 2007) which enables accretion on the disk orbital timescale rather than on the viscous timescale.

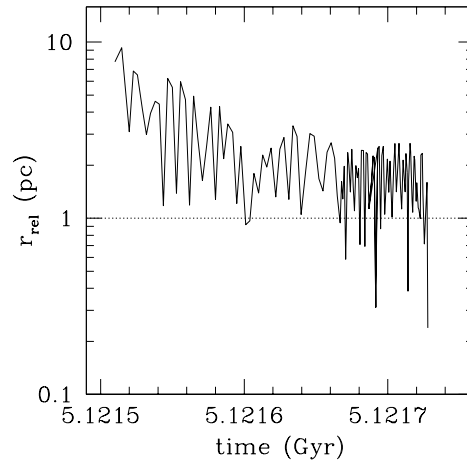


Fig. 5. Orbital evolution of the two SMBHs as a function of time in a multi-scale, merger simulation with a resolution of 0.1 pc in the gas component. Results are presented for an equation of state with $\gamma = 7/5$. The relative separation of the two SMBHs oscillates between ~ 0.5 pc and ~ 2 pc and never reaches the resolution limit of the simulation. As a result of very strong gas inflows, the density of the surrounding gas decreases considerably reducing the effect of dynamical friction on the SMBHs.

By the time the two black holes reach a separation of about 1 pc the central clump has already formed, sweeping most of the mass from the inner disk. As a result of the central inflow, the density of the surrounding gas decreases by a factor of ~ 5 . The density reduction weakens the effect of dynamical friction. We note that a similar phenomenon is seen by Dotti et al. (these proceedings). In their simulations, the disk profile becomes flatter rather than steeper, but it is still the case that the black holes find themselves in a region of very low density and reduced dynamical friction (the so-called “core”).

In addition, because the two black holes are orbiting around the central massive clump, their relative velocity is a factor of ~ 3 higher compared to that in the standard 2 pc simulation in which the central clump was not resolved. The dynamical friction force scales as ρ/v_{BH}^2 . The combined reduction of ρ and increase of v_{BH} results in an overall decrease of

almost a factor of 50 in the strength of dynamical friction, explaining the observed suppression in the orbital decay by almost two orders of magnitude. Moreover, as a result of the clump formation, the mass contained within the orbit of the two black holes has become much larger than the sum of their masses; the two black holes do not form a binary as in the 2 pc resolution simulations but only a loose pair.

Should we trust the formation of the massive clump and the suppression in the orbital decay? Probably not. Gas inflows are expected in non-axisymmetric disks, and they are indeed reported in high-resolution simulations of nuclear disks starting from equilibrium conditions (Escala 2006; 2007; Kawakatu and Wada 2008). Yet the magnitude of the inflows, hence the mass of the central clump and associated variation of the disk density profile, is likely exaggerated by the crude modeling of the ISM, and even more by the lack of star formation, supernovae feedback, and gas accretion onto the SMBHs. We take a closer look at this issue below. In Escala (2006; 2007) and Kawakatu & Wada (2008) the mass that collects in the inner parsec after a few million years is less than 1% of the total mass of the nuclear disk, while it is nearly 10% in our simulations (we note, however, that our nuclear disk is more than an order of magnitude more massive than the disk models used in these studies, hence stronger non-axisymmetric torques are expected due to the stronger self-gravity).

References

- Adams, F., et al. 1989, *ApJ*, 347, 959
 Bate, M. R., & Burkert, A. 1997, *MNRAS*, 288, 1060
 Barnes, J. E. & Hernquist, L. 1996, *ApJ*, 471, 115
 Begelman, M. C., Blandford, R. D. & Rees, M. J. 1980, *Nature*, 287, 307
 Berczik, P., Merritt, D., Spurzem, R., & Bischof, H. 2005, *ApJ*, 633, 680
 Blumenthal, G. R., Faber, S. M., Primack, J. R., & Rees, M. J. 1984, *Nature*, 311, 517
 Colpi, M., Mayer, L. & Governato, F. 1999, *ApJ*, 525, 720
 Davies, R. I., Tacconi, L. J., & Genzel, R. 2004, *ApJ*, 613, 781
 Dotti, M., Colpi, M., Haardt, F., & Mayer, L. 2007, *MNRAS*, 379, 956
 Dotti, M., Colpi, M., & Haardt, F. 2006, *MNRAS*, 367, 103
 Downes, D. & Solomon, P. M. 1998, *ApJ*, 507, 615
 Escala, A. 2007, *ApJ*, 671, 1264
 Escala, A. 2006, *ApJ*, 648, L13
 Escala, A., et al. 2005, *ApJ*, 630, 152
 Escala, A., et al. 2004, *ApJ*, 607, 765
 Fathi, K., et al. 2006, *ApJL*, 641, L25
 Ferrarese, L., & Ford, H. C. 2005, *Space Sci. Rev.*, 116, 523
 Kawakatu, N., & Wada, K. 2008, *ApJ*, 681, 73
 Kazantzidis, S., et al. 2005, *ApJL*, 623, L67
 Khochfar, S. & Burkert, A. 2006, *A&A*, 445, 403
 Klypin A., Zhao H. & Somerville R. S. 2002, *ApJ*, 573, 597
 Krumholz, M. R., Klein, R. I., & McKee, C. F. 2007, *ApJ*, 656, 959
 Mayer, L., Kazantzidis, S., Madau, P., Colpi, M., Quinn, T., & Wadsley, J. 2007, *Science*, 316, 1874
 Milosavljević, M. & Merritt, D. 2001, *ApJ*, 563, 34
 Ostriker, E. 1999, *ApJ*, 513, 252
 Spaans, M., & Silk, J. 2000, *ApJ*, 538, 115
 Springel, V., Di Matteo, T., & Hernquist, L. 2005, *MNRAS*, 361, 776
 Wada, K., & Norman, C. A. 2002, *ApJ*, 566, L21
 Wadsley, J. W., Stadel, J., & Quinn, T. 2004, *New Astronomy*, 9, 137